Journal Name

COMMUNICATION

Effect of chemical substitution on the construction of boroxine-based supramolecular crystalline polymers featuring B←N dative bonds

Subhrajyoti Bhandary,[a] Rahul Shukla,[b] and Kristof Van Hecke[a]*

Received 00th January 20xx,
Accepted 00th January 20xx

DOI: 10.1039/x0xx00000x

www.rsc.org/

We report the mechanochemical synthesis of five single-crystalline phenylboroxine and 1,4-diazabicyclo[2.2.2]octane (DABCO) ligand-based adducts, directed by boron-nitrogen dative bonds. By tuning the electronic features of the phenylboroxines by chemical modifications (-H/-OMe/-F/-Cl/-Br) at the *para*-position, the formation of the resulting bicomponent adducts can be controlled to obtain molecular to 1D polymeric crystalline materials. The electrostatic and quantum topological aspects of the B←N bonds reveal the origin for the different binding modes of the boroxine-DABCO adducts yielding molecular to polymeric structures.

The rational design and controllable synthesis of functional solid networks is one of the fundamental goals of materials science and crystal engineering.[1-2] Within the toolbox of crystal engineering, various weak non-covalent interactions have been utilized to connect molecular building blocks to achieve ordered network materials for gas storage,[3] separation,[4] catalysis,[5] and optoelectronic[6] applications. In this regard, weak but directional supramolecular interactions, such as hydrogen/halogen bonding and stacking interactions, could be a good alternative to robust metal-carbon coordinate bonds.[7-9] However, the stability of such weak supramolecular interactions, based on network materials, may be an issue when it comes to processability.

Organoboron-based crystalline materials have always drawn special attention in chemical science.[10] Particularly, organic boroxine compounds, containing a B_3O_3 core, were found to be promising for storage and optoelectronic applications.[10g,h] Recently, the B←N dative bond has appeared to serve as a good alternative to traditional non-covalent and metal-coordinate bonds, to build supramolecular network/host-guest-based crystalline assemblies, for various applications.[11-20] In general, the donation of electrons from the N-donor ligand to the electron-deficient boron atom (empty *p*-orbital) stabilizes such type of bonding. It has also been observed that the electronic properties of the interacting partner strongly influence the strength of the B←N dative bond.[12,14] The Severin group first reported on the relative interplay of B-N bonds in multi-dimensional crystalline polymers[11] and organic cages,[12] by changing electronic as well steric factors of different boronate esters and N-donor ligands. They also utilized such flexible B←N linkages to build porous crystalline polymers.[18] Hence, it is of great interest to understand the structural and quantum topological aspects of B←N bonds, in different crystalline and chemical environments for further development of transition metal-free functional materials. With this purpose, we have now synthesized different chemically modified (by electron-donating and withdrawing substituents) molecular crystals and 1D crystalline networks, stabilized by B←N dative bonds.

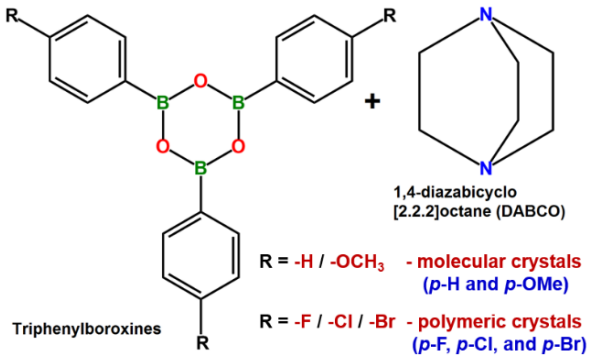

Scheme 1. Chemical structure of *para*-substituted boroxines (R = -H/-OCH3/-F/-Cl/-Br) and type of crystalline adducts formed with DABCO (their respective codes are depicted in blue color.

[a] XStruct, Department of Chemistry, Ghent University. Krijgslaan 281-S3, B-9000-Ghent, Belgium, E-mail: kristof.vanhecke@ugent.be.
[b] Department of Chemistry, Ben-Gurion University of the Negev, Beer Sheva, 841051, Israel.

† Electronic Supplementary Information (ESI) available: Experimental details of mechanochemical synthesis and crystal growth; Powder X-ray diffraction and single-crystal structure determination; Computational details. CCDC 2131638-2131642 contain the supplementary crystallographic data for this paper. These data can be obtained free of charge from The Cambridge Crystallographic Data Centre via www.ccdc.cam.ac.uk/structures. For ESI and crystallographic data in CIF or other electronic format see DOI: 10.1039/x0xx00000x.

Journal Name

COMMUNICATION

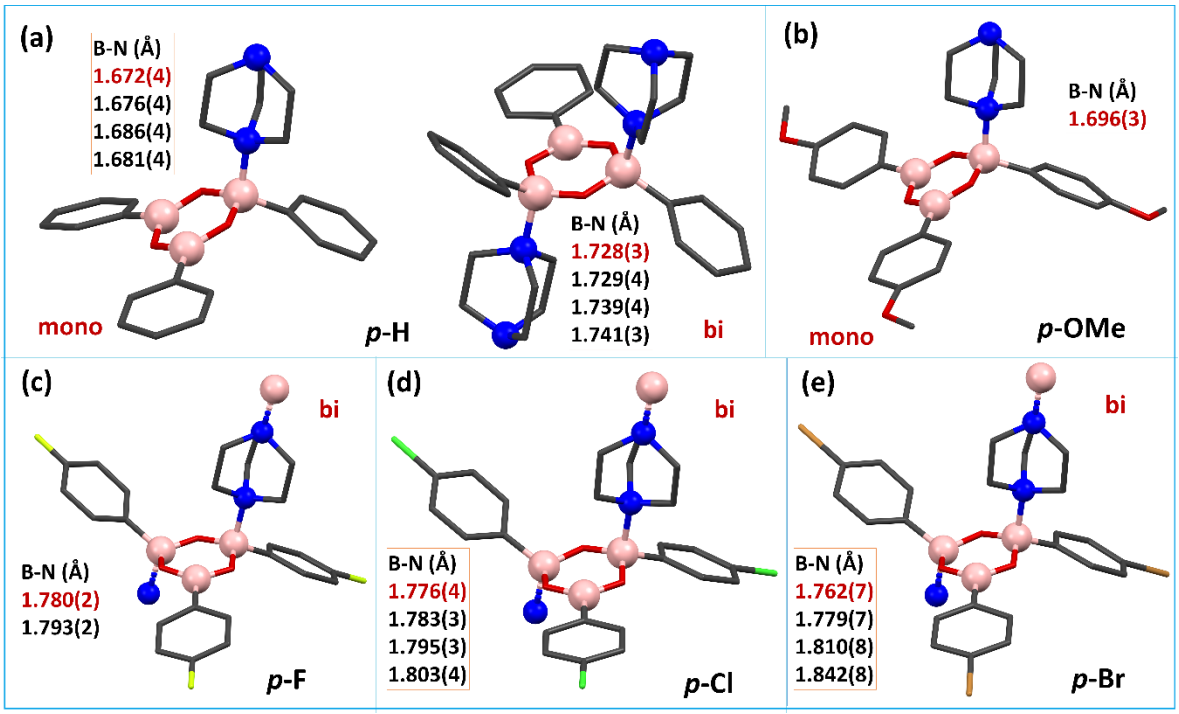

Fig. 1 Representative crystal structures of differently *para*-substituted phenylboroxines and DABCO adducts. (a) *p*-H and (b) *p*-OMe show molecular crystal structures, having mono and bicoordinated DABCO ligands. (c-e) All halogen-substituted (*p*-F, *p*-Cl, and *p*-Br) polymeric crystal structure adducts exhibit bicoordinated DABCO ligands. The observed shortest B-N bond distances in each crystal structure are highlighted in red. Note that multiple molecules are observed in the asymmetric unit of the crystal structures of *p*-H, *p*-Cl, and *p*-Br.

In this communication, we present a series of five crystalline adducts (Scheme 1), based on differently *para*-substituted phenylboroxines (-H/-OCH_3/-F/-Cl/-Br) and the ditopic 1,4-diazabicyclo[2.2.2]octane ligand (DABCO). The mechanochemical dry grinding (manual) method was employed for the synthesis of all adducts by combining chemically functionalized boroxines and DABCO molecules (see ESI for experimental details). The final products were characterized by both powder X-ray diffraction and single-crystal X-ray diffraction (SCXRD) analyses (Fig. S1-S2). The conditions for single crystal growth and crystallographic data are provided in the ESI (Tables S1-S2).

The SCXRD investigation revealed that both -H and -OCH_3 substituted phenyl boroxines bind to DABCO ligands (mono/bicoordinated, and monocoordinated fashion, respectively) forming molecular crystals (Fig. 1 and Table S2), whereas the three halogen-substituted derivatives (-F/-Cl/-Br) yield supramolecular polymeric (bicoordinated) adducts. In all five structures, chemically functionalized boroxines are connected with N-donor DABCO ligands *via* B←N dative bonds, which show varying distances. In the case of the unsubstituted adduct (*p*-H, $P2_1/n$, Z' = 4+2) a complex but interesting interplay of multiple (six) crystallographic independent molecules, is observed (Fig. 1a and S2a). In fact, the asymmetric unit contains four molecules of mono-coordinated adducts (one B-N bond each) and two molecules of bicoordinated adducts (two B-N bonds each). The shortest B-N bond distances among all *p*-H molecules vary from 1.672(4) Å (for mono) to 1.728(3) Å (bi). The supramolecular features of the -OCH_3 substituted adduct (*p*-OMe, $P2_1/n$, Z' = 1) demonstrate that the ditopic DABCO ligand is mono-coordinated to the phenylboroxine core (Fig. 1b) *via* one B←N dative bond (1.696(3) Å). In contrast, the introduction of halogens on the phenylboroxines resulted all in supramolecular polymeric structures (Fig. 1c-e). In the *p*-F substituted adduct (*p*-F, *C*2/c, Z' = 1), one boroxine core is attached to two coordinating, bridging DABCO ligands, which connect the boroxine cores, to form a 1D polymeric chain of B←N dative bonds, having a shortest B-N distance of 1.780(2) Å (Fig. 1c). A similar 1D polymeric chain of B←N dative bonds is also observed for *p*-Cl (*P*-1, Z' = 2) and *p*-Br (*P*-1, Z' = 2) substituted adducts, with shortest B-N distances of 1.776(4) Å and 1.762(7) Å, respectively. Furthermore, it is important to

state that the crystal lattices of all three supramolecular polymers (*p*-F, *p*-Cl, and *p*-Br) contain guest solvent molecules in the solvent-accessible voids within their B←N networks (Fig. 2). Solvent-accessible void volumes range from 114 Å^3 to 149 Å^3 per unit cell (using a probe radius of 1.2 Å) after removing the solvents.

The phenylboroxine-DABCO binding modes through B←N bonds in all crystalline adducts and their influence on the formation of various molecular to polymeric structures can be rationalized through assessing the electronic features of the chemically modified phenylboroxine cores. To obtain the change in electronic distribution upon chemical substitution, we mapped molecular electrostatic potentials (ESP) of gas-phase optimized[21] [at the B3LYP-D3/6-311+g(d,p) level of theory]

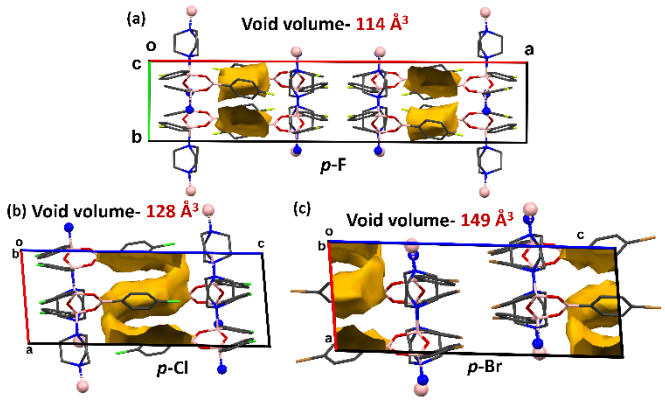

Fig. 2 Supramolecular networks of the three halogen-substituted crystals (*p*-F, *p*-Cl and *p*-Br) showing solvent-accessible voids (yellow surfaces) in their unit cells. The void space in the lattices was calculated using CCDC Mercury[22] (version 2020.3.0), using a probe radius of 1.2 Å and grid spacing of 0.7 Å.

parent phenylboroxines (BO-H, BO-OMe, BO-F, BO-Cl, and BO-Br) and DABCO molecules (Fig. 3). The ESP map of the unsubstituted phenylboroxine (BO-H) depicts a high electron-deficient surface (blue region of B_3O_3 ring in Fig. 3a) near the B-atoms having a positive potential of 65.6 kJ/mol. The phenyl rings exhibit a negative (red) surface (-55.1 kJ/mol) on the account of having aromatic electron density. Upon substitution of *para*-H by the electron-donating –OCH_3 group (Fig. 1b), the positive ESP surface on the B-atoms becomes less electron-depleted (47.3 kJ/mol). When H-atoms are replaced by halogens in the phenylboroxines (BO-F, BO-Cl, and BO-Br), their ESP surfaces change to highly positive at the B-sites, in comparison to unsubstituted BO-H (deep blue surface in Fig. 3c-e). The ESPs of their phenyl rings show mild electronegative character as depicted by white surfaces. This is due to the electron-withdrawing effect of the halogen (F/Cl/Br) substituents, attached to the three phenyl rings. The depletion of electron density (ESP values) at the B-atoms increases to a maximum of 91.9 kJ/mol for BO-F. In contrast, the center of the DABCO molecules has a highly negative ESP (deep red, -141.8 kJ/mol) due to the presence of electron donor N-atoms (Fig. 3f). Hence, in general, it can be concluded that the affinity of binding DABCO molecules to different phenylboroxines *via* B←N bonds is electrostatically favorable as reflected from their strong complementarity in their ESP surfaces. In particular, it can be reasoned, on the one hand, that relatively less (in BO-OMe) to moderate (BO-H) electrostatically complement B-atoms, concerning the N-ligand, account for the mono-coordinated and mono/bicoordinated DABCO (B←N) forming *p*-OMe and *p*-H molecular crystals, respectively. While on the other hand, the electron-withdrawing effect of different halogens strongly enhances the electrostatic complementarity between corresponding phenylboroxines (BO-F, BO-Cl, and BO-Br) and DABCO molecules. In effect, such electron-withdrawing substituents favor the formation of an infinite chain of B←N bonds and subsequent polymeric crystal structures (*p*-F, *p*-Cl, and *p*-Br).

The topological features of B←N dative bonds and their variations in different chemical environments (substituent

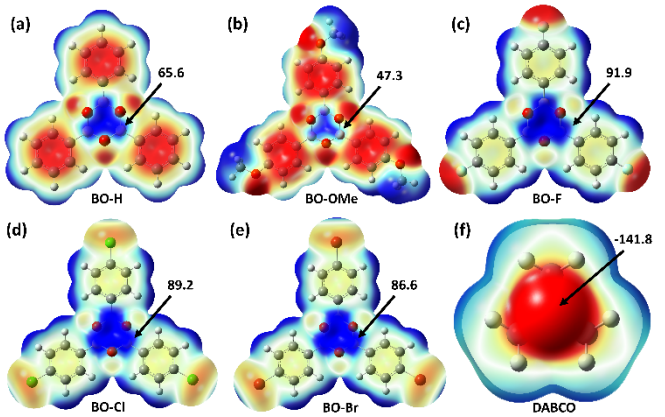

Fig. 3 Molecular electrostatic potentials (ESP) mapped on the gas phase optimized geometries [computed at the B3LYP-D3/6-311+g(d,p) level of theory] for isolated phenylboroxines with a color scale of < -49.9 kJ/mol (all red) to > 49.9 kJ/mol (all blue). ESP values (in kJ/mol) of the B and N sites are indicated (black arrow).

variant crystals) have been quantified by the quantum theory of atoms in molecules (QTAIM) method.[23-24] The QTAIM provides a direct and trustworthy mapping of chemical bonds by describing the distribution of electron density in crystals. In a previous study, the bonding situation of B-N coordination, in relatively simpler model systems, was described to show both a covalent and electrostatic character.[25-26] Therefore, QTAIM derived bonding descriptors in Lewis acid and base type B-N stabilized molecular and polymeric crystals, would be certainly interesting. We have isolated all shortest B←N bonds observed in the five crystalline adducts and investigated their topological properties at the bond critical point (BCP), such as electron density (ρ), Laplacian of electron density ($\nabla^2\rho$), and bond dissociation energy (D.E^v). It must be noted that the observed smallest B-N distances in the crystal structures range from 1.672(4) Å (for *p*-H) to 1.780(2) Å (for *p*-F), which is larger than for a classical covalent distance and too short for any van der Waals interactions. Such distance range lies in the category of 'short' B-N dative bond structures.[27] The topological analysis has been performed at the B3LYP-D3/6311+g(d,p) level of theory. Such analyses depict the presence of (3,-1) BCPs between B-N atoms and positive values of $\nabla^2\rho$ (ranging from 1.9290-4.6652 e/Å^5), which is indicative of *closed-shell* bonding

interactions (red circles Fig. 4). The ρ associated with the BCP of all B-N bonds are in the range of 0.6361-0.7760 e/Å^3. Interestingly, significantly higher values of ρ and $\nabla^2\rho$ (Fig. 4) have been realized for two B-N monocoordinated molecules (*p*-H and *p*-OMe), in comparison to those of all bicoordinated adducts (*p*-H, *p*-F, *p*-Cl, and *p*-Br). It is obvious that the electron-withdrawing effect of halogens increases the deficiency of electron density around the B- periphery, and subsequently B-N bonds exhibit reduced values of ρ and $\nabla^2\rho$ in the three halogenated crystals (*p*-H, *p*-F, *p*-Cl, and *p*-Br). However, this deficiency of electron density at B-regions drives the formation of polymeric adducts by infinite B-N coordination due to the electrostatic effects. Another intriguing topological factor, the electron delocalization index (DI)[28] indicates the multiplicity of a chemical bond. The DI of a B-N dative bond can be described as the average number of delocalized electrons between

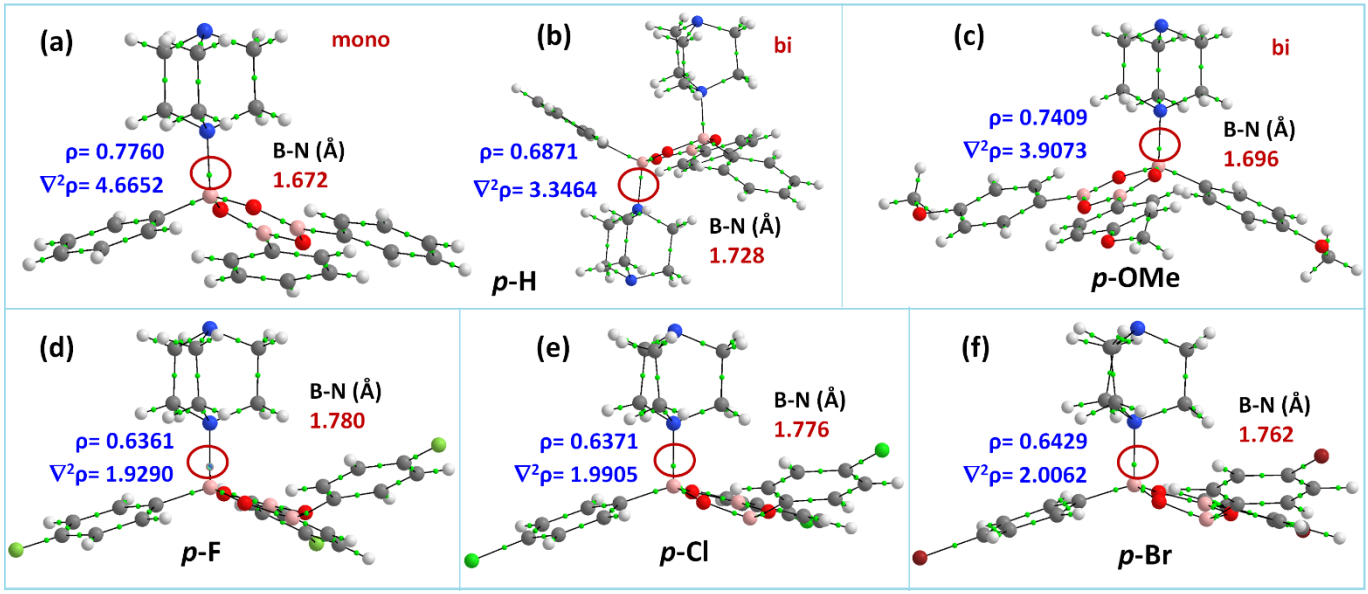

Fig. 4 Representative molecular graphs corresponding to the observed shortest B-N distances (in red color) in each crystalline adduct (a-f), showing the distribution of BCPs (green dots). Red circles indicate BCPs for B-N bonds and values of their ρ (e/Å^3) and $\nabla^2\rho$ (e/Å^5) are given (in blue color).

Table 1. Electron delocalization index and bond dissociation energies (QTAIM derived) of all shortest B-N bonds, based on the five reported crystal structures

B-N bonds in crystal adducts	Electron delocalization index (DI)	Dissociation energy (D.E^v), kJ/mol.
p-H (1.672 Å)	0.283	288.3938
p-H (1.728 Å)	0.260	239.0539
p-OMe (1.696 Å)	0.284	266.6185
p-F (1.780 Å)	0.257	204.9134
p-Cl (1.776 Å)	0.257	205.8324
p-Br (1.762 Å)	0.260	208.3004

quantum B and N atoms. The computed DI of shortest B-N bonds in all adducts are in the range of 0.257 (for *p*-F and *p*-Cl) to 0.284 (for *p*-OMe), which suggests a single bond type[26] (number of delocalized electron pairs is less than 1) character of the dative bond (Table 1). Furthermore, the energetics of all B-N bonds were quantified through the QTAIM derived D.E^v (ranging from 204.9134 to 288.3938 kJ/mol). The relatively lower values of D.E^v (Table 1) of B-N bonds for all polymeric crystals (*p*-F, *p*-Cl, and *p*-Br) could be the consequence of the electron-withdrawing effect of the substituents, attached to the phenyl rings.

To rationalize the efficacy and robustness of the dative B←N bond in crystalline supramolecular polymerization and crystal engineering, we performed a Cambridge Structural Database (CSD, version 5.42)[29] search. The database investigation resulted in the occurrence of only 31 polymeric metal-free crystal structures, featuring B←N bonds (see ESI). This clearly shows that such a dative bond could provide a new tool in crystal engineering. Therefore, the B←N bond could be further explored as well as utilized in the design and construction of organoboron-based metal-free crystalline supramolecular frameworks with functional properties.

In summary, we have described the mechanochemical synthesis and characterization of five substituent variants of molecular to 1D supramolecular network materials of *para*-functionalized phenylboroxine-DABCO adducts formed by B←N dative bonds. The electron-donating (-OMe) and unsubstituted phenylboroxines favor the formation of molecular crystals, whereas supramolecular polymers are obtained due to strong electron withdrawal effects from the halogen (-F/-Cl/-Br) substituents. This is further rationalized by the strong electrostatic complementarity that exists between the electron-deficient boron surrounding in the chemically modified phenylboroxines and the N-donor DABCO ligand. An in-depth QTAIM analysis unequivocally establishes the electron density-dependent topological parameters of the B←N single bond observed in different chemical environments of all crystalline adducts. The topological features of *closed-shell* type B←N bonds further suggest that the presence of electron-withdrawing substituents (-F/-Cl/-Br) on the phenyl rings noticeably decreases the participation of electron density and Laplacian of electron density between B and N atoms. Such

effects lead to the formation of polymeric B←N chains in crystal environments. Finally, this study provides a fundamental understanding of less exploited B←N bonds in crystalline materials. As such, transition metal-free supramolecular-ordered materials with diverse functional properties could be designed and executed in the future through B←N bond-directed crystal engineering principles.

S.B. and K.V.H. acknowledge the Research Foundation - Flanders (FWO) for funding (Project No. 1275221N). R.S. thanks the Kreitman Foundation for a postdoctoral fellowship. We also thank Prof. Sebastian Kozuch for providing us access to the computational facility. We acknowledge the help of Laurens Bourda for powder X-ray diffraction measurements.

Author contributions

K.V.H. designed and supervised the project. S.B. performed all experiments and analyzed preliminary results. R.S. executed computational calculations. The manuscript was written from the contributions of all authors.

Conflicts of interest

"There are no conflicts to declare".

Notes and references

1 G. R. Desiraju, J. J. Vittal and A. Ramanan, *Crystal Engineering*: A Textbook, World Scientific, Singapore, 2011.

2 P. J. Waller, F. Gándara and O. M. Yaghi, *Acc. Chem. Res*., 2015, **48**, 3053.

3 S. T. Kostakoğlu , Y. Chumakov , Y. Zorlu , A. E. Sadak , S. Denizalti , A. G. Gürek and M. M. Ayhan , *Mater. Adv*., 2021, **2**, 3685.

4 W.-Q. Tang, Y.-J. Zhao, M. Xu, J.-Y. Xu, S.-S. Meng, Y.-D. Yin, Q.-H. Zhang, L. Gu, D.-H. Liu and Z.-Y. Gu, *Angew. Chem., Int. Ed.*, 2021, **60**, 6920.

5 K. T. Mahmudov, M. N. Kopylovich, M. F. C. G. da Silva and A. J. L. Pombeiro, *Noncovalent Interactions in Catalysis*, RSC, 2019, https://doi.org/10.1039/9781788016490

6 A. Leventis, J. Royakkers, A. G. Rapidis, N. Goodeal, M. K. Corpinot, J. M. Frost, D. K. Bučar, M. O. Blunt, F. Cacialli and H. Bronstein, *J. Am. Chem. Soc*., 2018, **140**, 1622.

7 P. Li, M. R. Ryder and J. F. Stoddart, *Acc. Mater. Res*., 2020, **1**, 77.

8 G. Berger, J. Soubhye and F. Meyer, *Polym. Chem*. 2015, **6**, 3559.

9 (a) X. Li, J. Qiao, S. W. Chee, H.-S. Xu, X. Zhao , H. S. Choi, W. Yu , S. Y. Quek, U. Mirsaidov and K. P. Loh, *J. Am. Chem. Soc*., 2020, **142**, 4932; (b) S. Bhandary and D. Chopra, *Cryst. Growth Des*., 2018, **18**, 3027.

10 (a) J. W. B. Fyfe and A. J. B. Watson, *Chem*, 2017, **3**, 31; (b) T. Faury, F. Dumur , S. Clair, M. Abel, L. Porte and D. Gigmes , *CrystEngComm*, 2013, **15**, 2067; (c) J. Drapała, P. H. Marek-Urban, P. Klimkowski, K. A. Urbanowicz, K. Gontarczyk, K. Woźniak, S. Luliński and K. Durka, *CrystEngComm*, 2021, **23**, 8169; (d) L. Fornasari, S. d'Agostino and D. Braga, *CrystEngComm*, 2019, 21, 3186; (e) G. Campillo-Alvarado, C. A. Staudt, M. J. Bak and L. R. MacGillivray, *CrystEngComm*, 2017, **19**, 2983; (f) R. Nishiyabu, Y. Kubo, T. D. James and J. S. Fossey, *Chem. Commun*., 2011, **47**, 1124; (g) J. L. Mendoza-Cortés, S. S. Han, H. Furukawa, O. M. Yaghi and W. A. Goddard, *J. Phys. Chem. A*, 2010, **114**, 10824; (h) G. Alcaraz, L. Euzenat, O. Mongin, C. Katan, I. Ledoux, J. Zyss, M. Blanchard-Desce and M. Vaultier, *Chem. Commun*., 2003, 2766.

11 E. Sheepwash, V. Krampl, R. Scopelliti, O. Sereda, A. Neels and K. Severin, *Angew. Chem., Int. Ed*., 2011, **50**, 3034.

12 B. Icli , E. Sheepwash , T. Riis-Johannessen , K. Schenk , Y. Filinchuk , R. Scopelliti and K. Severin , *Chem. Sci*., 2011, **2**, 1719.

13 E. Sheepwash, N. Luisier, M. R. Krause, S. Noé, S. Kubik and K. Severin, *Chem. Commun*., 2012, **48**, 7808.

14 N. Luisier, K. Bally, R. Scopelliti, F. T. Fadaei, K. Schenk, P. Pattison, E. Solari and K. Severin, *Cryst. Growth Des*., 2016, **16**, 6600.

15 B. Icli, E. Solari , B. Kilbas, R. Scopelliti and K. Severin, *Chem. – Eur. J*., 2012, **18**, 14867.

16 A. Torres-Huerta, M. J. Velásquez-Hernández, D. Martínez-Otero, H. Höpfl and V. Jancik , *Cryst. Growth Des*., 2017, **17**, 2438.

17 J. Cruz-Huerta, G. Campillo-Alvarado, H. Höpfl, P. Rodríguez-Cuamatzi, V. Reyes-Márquez, J. Guerrero-Álvarez, D. Salazar-Mendoza and N. Farfán-García*, Eur. J. Inorg. Chem*., 2016, **355**.

18 A. J. Stephens , R. Scopelliti , F. F. Tirani , E. Solari and K. Severin , *ACS Mater. Lett*., 2019, **1**, 3.

19 G. Campillo-Alvarado, K. P. D'mello, D. C. Swenson, S. V. Santhana Mariappan , H. Höpfl, H. Morales-Rojas and L. R. MacGillivray, *Angew. Chem., Int. Ed*., 2019, **58**, 5413.

20 G. Campillo-Alvarado, E. C. Vargas-Olvera, H. Höpfl, A. D. Herrera-España, O. Sánchez-Guadarrama, H. Morales-Rojas, L. R. MacGillivray, B. Rodríguez-Molina and N. Farfán, *Cryst. Growth Des*., 2018, **18**, 2726.

21 All gas phase calculations were performed using Gaussian 16. See ESI for details.

22 C. F. Macrae, I. Sovago, S. J. Cottrell, P. T. A. Galek, P. McCabe, E. Pidcock, M. Platings, G. P. Shields, J. S. Stevens, M. Towler and P. A. Wood, *J. Appl. Cryst*., 2020, **53**, 226-235.

23 R. F. W. Bader, Atoms in Molecules: A Quantum Theory, Oxford University Press, Oxford, U.K., 1990.

24 V. G. Tsirelson, *The Quantum Theory of Atoms in Molecules: From Solid State to DNA and Drug Design*, ed. C. F. Matta, R. J. Boyd, Wiley-VCH, Weinheim, Germany, 2007, ch. 10. 45.

25 S. Mebs , S. Grabowsky , D. Förster , R. Kickbusch , M. Hartl , L. L. Daemen , W. Morgenroth , P. Luger , B. Paulus and D. Lentz *, J. Phys. Chem. A*, 2010, **114**, 10185.

26 G. Mierzwa , A. J. Gordon and S. Berski , *J. Mol. Model*., 2020, **26**, 1.

27 A. Nandi, N. Tarannam, D. Rodrigues Silva, C. Fonseca Guerra, T. A. Hamlin and S. Kozuch, *ChemPhysChem*, 2021, **22**, 1857.

28 R. F. W. Bader, C. F. Matta and F. Cortés-Guzmán, *Organometallics*, 2004, **23**, 6253.

29 C. R. Groom, I. J. Bruno, M. P. Lightfoot and S. C. Ward, *Acta Cryst*., 2016, **B72**, 171.

Table of contents

B←N dative bond-associated molecular to polymeric crystals have been synthesized by tuning their electronic features. The supramolecular and quantum crystallographic aspects of the B←N dative bonds were thoroughly investigated.